XLVI CILAMCE
VITÓRIA - ES - BRAZIL - 2025
XLVI IBERO-LATIN AMERICAN CONGRESS ON COMPUTATIONAL METHODS IN ENGINEERING

Dynamic Response of a Rotor Interacting with a Periodic Foundation Supported by the Soil

Amauri C. Ferraz[1], Luis F. V. Lima[1], Euclides Mesquita[1]

1Dept. of Computational Mechanics, University of Campinas
200 Mendeleyev St, 13083-970, Campinas SP, Brazil
amauriferrazz@gmail.com, lfvl_@hotmail.com, euclides@fem.unicamp.br

Abstract. The dynamic response of mechanical systems depends largely on the boundary conditions prescribed to the system. The rotor's response is strongly affected by its supporting system, which governs both stationary and transient behavior. On the other hand, much research has been done on the filtering properties of periodic structures. The current paper discusses a system composed of a rotor, a structure and a periodic foundation supported by the soil. The main idea is to investigate the behavior of this complex system in frequencies where the periodic structure presents a 'band gap'. The article will address the possibilities of isolating the rotor-structure dynamic behavior from that of soil, in given frequency ranges. The soil is modeled by the Boundary Element Method, and the structure is linear and described by the Finite Element Method. The rotor is a Laval-Jeffcott rotor presenting internal and external damping mechanisms. The excitation applied to the system is a constant value of torque. The question to be addressed is whether the periodic structure can isolate the rotor system from the soil response for the two mentioned excitation mechanisms.

Keywords: dynamics of rotors and structures, periodic structures, soil dynamics.

1 Introduction

Rotor-foundation systems interacting with soil exhibit complex dynamics due to radiation and geometric damping effects inherent to soil behavior. Kellezi and Hansen [1] addressed this by performing time-domain dynamic analysis of offshore wind turbines using a 3D axisymmetric transient finite element model incorporating radiation damping via absorbing boundaries and soil nonlinearity to assess foundation responses. Recently, periodic foundations have gained attention for vibration isolation, with studies such as Xiang et al. [2] demonstrating frequency bandgaps that effectively attenuate structural vibrations. Coupled-field dynamic problems are commonly solved via partitioned methods, where subsystems with weak coupling or different time scales are analyzed separately. Felippa and Park [3] detail iterative staggered coupling strategies that sequentially integrate single-field solvers, enhancing modularity and efficiency. The Boundary Element Method (BEM) is extensively applied in dynamic soil-structure interaction (DSSI), particularly in the frequency domain, due to its natural representation of geometric damping from energy-radiating waves, as observed in the study of Carrion and Mesquita [4].

Ferraz et al. [5] proposed a transient analysis methodology for soil-foundation-structure systems including rotor dynamics, modeling a Laval rotor on a rigid base supported by a frame over a viscoelastic half-space. Their approach simulates the coupled system's transient response during the rotor run-up phase, capturing resonance crossings that amplify displacements and energy dissipation, potentially causing rotor stall and system failure if dissipated energy exceeds input torque. This study replaces the structural frame with a periodic foundation to evaluate its effect on rotor-soil interaction dynamics. Four configurations are analyzed, a rotor on homogeneous or periodic foundations with either fixed base or viscoelastic half-space support, focusing on the torque required to overcome resonance during run-up.

2 Formulation

Figure 1a shows the rotor-foundation-soil system analyzed using the proposed methodology, consisting of a Laval rotor on a rigid foundation coupled to a periodic foundation over a 3D viscoelastic half-space. The model is partitioned at the rotor-foundation/periodic-foundation interface, with the equations of motion for the rotor-rigid-foundation (Fig. 1b) and soil-periodic-foundation (Fig. 1c) subsystems integrated in the time domain. Interaction is addressed through an iterative coupling procedure ensuring dynamic compatibility, and excitation is introduced via an external torque on the rotor shaft.

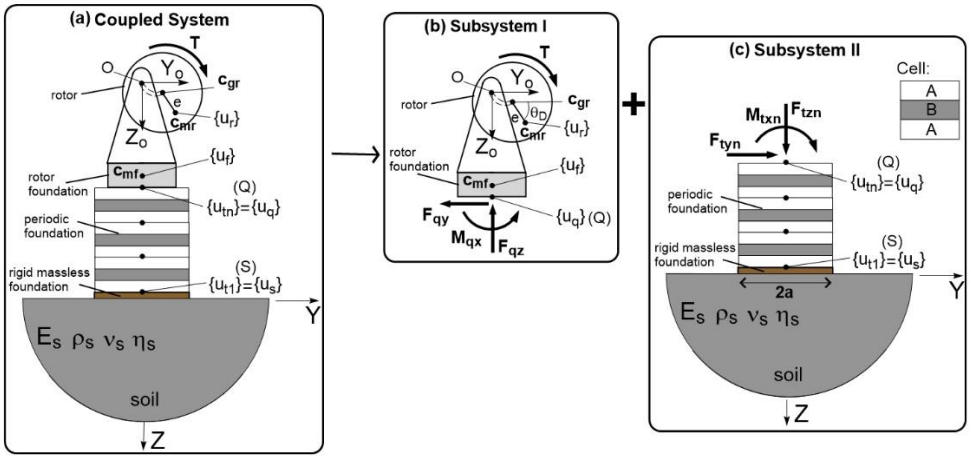


Figure 1. Decomposition of rotor-foundation-soil system

The rotor subsystem has three degrees of freedom (DOFs): vertical, horizontal, and angular, defined as $\{u_r\}=\{u_{rz},u_{ry},\theta_D\}$. The rigid foundation DOFs are $\{u_f\}$, and each node *i* of the periodic foundation has $\{u_{ti}\}$. In this study, only vertical DOFs are considered for all components, and the rotor's angular DOF is also included.

2.1 Rotor-rigid-foundation subsystem modeling

Figure 1b presents the rotor-rigid-foundation subsystem, modeled as a Jeffcott (Laval) rotor with rigid bearings. The model consists of an elastic shaft with an unbalanced disk (m_D) located at the geometric center of the shaft (c_{gr}). Both internal (c_I) and external (c_E) damping coefficients are included in the model. The displacement of the rotor's center of mass (c_{mr}) is expressed as the superposition of the displacement of the geometric center of the rotor (u_{rz}) and the relative displacement between the c_{gr} and the c_{mr} (eccentricity *e*). Thus, the total displacement component in z-direction is defined as $p^{D/O} = u_{rz} + e\sin\theta_D$. The rigid foundation displacement at the interface with the soil-periodic-foundation subsystem (Q) is given by u_{qz}. The shaft's elastic stiffness is represented by k_r. The excitation of the system is introduced through an external torque T applied to the rotor shaft. The linear equations of motion for rotor and its rigid foundation (eqs. (1) and (2), respectively), as well as the rotor's angular equation of motion (eq. (3)), are derived from the forces acting on the system. These include the rotor's elastic forces (F_{Er}), external damping (F_{Ar}), internal damping (F_{Ir}), weight (P_D), and torque (T); and the foundation forces, which comprise the reaction at the bearing ($F_{Er}+F_{Ar}+F_{Ir}+P_D$), the foundation's weight (P_F), and the interface forces with the periodic foundation (F_{qz},F_{qy},M_{qx}), as reported in Ferraz et al. [5]. The rotor's weight induces a static displacement u_{est}.

$$m_D(\ddot{u}_{rz} + \ddot{\theta}_D e\cos\theta_D - \dot{\theta}_D^2 e\,sen\,\theta_D) = (-c_E - c_I)\dot{u}_{rz} + (c_E + c_I)\dot{u}_{qz} - k_r u_{rz} + k_r u_{qz} \tag{1}$$

$$m_F\ddot{u}_{qz} = (c_E + c_I)\dot{u}_{rz} - (c_E + c_I)\dot{u}_{qz} + k_r u_{rz} - k_r u_{qz} + F_{qz} \tag{2}$$

$$I_{xx}^{I/D}\ddot{\theta}_D = (c_I + c_E)(-\dot{u}_{qz} + \dot{u}_{rz})e\cos\theta_D + (-u_{rz} + u_{qz} - u_{est})c_I\dot{\theta}_D e\,sen\,\theta_D + (u_{rz} + u_{est} - u_{qz})k_r e\cos\theta_D + T \tag{3}$$

2.2 Soil-periodic-foundation subsystem

Figure 1c shows Subsystem II, consisting of a periodic foundation (index *t*) connected to a viscoelastic half-space (index *s*) through a rigid, massless interface. Modeled using FEM with bar elements, each node *i* has a single DOF: $\{u_{ti}\}$. The bottom node $\{u_{t1}\}$ is kinematically coupled to the soil-foundation DOF $\{u_s\}$, representing the interface displacement, computed via the Direct Boundary Element Method (DBEM) in the frequency domain, following Carrion et al. [4]. External excitation is applied at the top node *n* as $\{F_{tn}\}$. Soil-foundation interaction enforces continuity $\{u_{t1}\}=\{u_s\}$ and equilibrium $\{F_{t1}\}+\{F_s\}=0$, as in the work of Pacheco et al. [6].

Remark 1: The periodic foundation. The periodic foundation consists of three identical ABA-type unit cells (Fig. 1c), composed of materials A and B, with each unit cell discretized into *m* elements. The mass and stiffness matrices of the bar elements are defined in eq. (4) by Cook et al. [7], where ρ is the material density, E is Young's modulus, A is the cross-sectional area, and L is the element length.

$$\left[m_{el}\right]=\frac{\rho AL}{6}\begin{bmatrix}2 & 1\\ 1 & 2\end{bmatrix} \quad ; \quad \left[k_{el}\right]=\frac{EA}{L}\begin{bmatrix}1 & -1\\ -1 & 1\end{bmatrix} \tag{4}$$

The complete equations of motion governing the periodic foundation are given by:

$$[M_t]_{n\times n}\{\ddot{u}_t(t)\}_{n\times 1}+[C_t]_{n\times n}\{\dot{u}_t(t)\}_{n\times 1}+[K_t]_{n\times n}\{u_t(t)\}_{n\times 1}=\{F_t(t)\}_{n\times 1} \tag{5}$$

Remark 2: The soil dynamic response. The soil dynamic response at the surface of the rigid and massless foundation is defined by eq. (6), where *a* is half the foundation width, G is the soil shear modulus, and $\{N_{Sz}(\omega)\}$ is the frequency-dependent flexibility vector. This vector relates the displacement in z-direction at point S, $\{U_{sz}(\omega)\}$, to the corresponding force vector $\{F_{sz}(\omega)\}$.

$$\{U_{sz}(\omega)\}=\frac{1}{Ga}\{N_{Sz}(\omega)\}\{F_{sz}(\omega)\} \tag{6}$$

Figure 2 shows the frequency dependence of the flexibility vector $\{N_{Sz}(\omega)\}$ of a homogeneous half space.

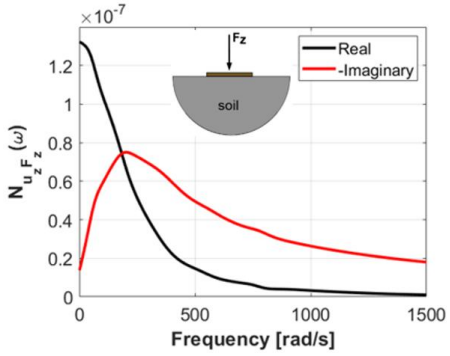


Figure 2. Flexibility of a rigid massless foundation on the surface of the half space

Remark 3: Coupling of the periodic foundation and soil dynamic response. Applying the Fourier Transform to eq. (5) and partitioning the result allows isolation of the response at the first node ($\{u_{t1}\}$) from the remaining structural nodes ($\{u_{tm}\}$), facilitating coupling with the response of the rigid and massless foundation on soil ($\{u_s\}$). The resulting equations, incorporating the influence of the soil on the periodic foundation, are derived from the manipulation of eqs. (5) and (6) and are given as follows:

$$\{U^*_{tm}(\omega)\}_{m\times 1}=[S_{str}(\omega)]_{m\times m}\{F_{tm}(\omega)\}_{m\times 1} \tag{7}$$

$$\{U^*_{t1}(\omega)\}_{1\times 1}=\{S_{soil}(\omega)\}_{1\times m}\{F_{tm}(\omega)\}_{m\times 1} \tag{8}$$

Matrix $[S_{str}(\omega)]$ and vector $\{S_{soil}(\omega)\}$, defined in eqs. (7) and (8), respectively, represent the periodic foundation's FRFs considering soil-structure interaction effects. When subjected to an external load vector $\{F_{tm}\}$, the frequency-domain response of all structural DOFs, $\{U^*_{t1}\}+\{U^*_{tm}\}$, can be determined.

The Rational Fraction Polynomial Method (RFPM), described by Ewins [9], allows the extraction of modal parameters of the modified FRFs of the soil-foundation system, and definition of a soil-influenced periodic foundation modal basis. This enables the formulation of orthogonal equivalent equations of motion in modal coordinates, as in the study of Ferraz et al. [8]:

$$[I]\{\ddot{q}_t(t)\} + [2\xi_n\omega_n]\{\dot{q}_t(t)\} + [\omega_n^2]\{q_t(t)\} = [\Phi]^T\{F_{tn}(t)\} \tag{9}$$

The physical response $\{u_t\}$ is obtained by transforming the modal coordinates $\{q_t\}$ via $\{u_t\}=[\Phi]\{q_t\}$.

2.3 Iterative coupling

After defining the equations of motion, the subsystems are coupled by the staggered solution method, as described in Felippa and Park [3], which enhances computational efficiency by eliminating iterative convergence at each time step.

$$F_{qz}(t)^{(n)} = -m_F\ddot{u}_{sz} + (c_E + c_I)\dot{u}_{rz} - (c_E + c_I)\dot{u}_{qz} + k_r u_{rz} - k_r u_{qz} \tag{10}$$

The coupling begins with the definition of a predictor term, comprising the interface force (F_{qz}), as defined in eq. (10). At the initial time step, this term is computed using the system's initial displacement and velocity conditions. For subsequent steps, it is updated based on the response at previous time step n. The predictor then acts as the excitation input for Subsystem II (Fig. 1c), allowing the calculation of linear displacements of soil-foundation subsystem at time step n+1 via eq. (9). These displacements are used to integrate the equations of motion of Subsystem I (rotor – Fig. 1b) at the same time step, as described in eqs. (1) to (3). The cycle continues by recalculating the predictor term for the next time step using eq. (10) with previous step data.

3 Numerical Results

The proposed methodology is applied to four rotor–foundation–soil configurations (Fig. 3). Cases *a* and *b* involve a fixed base with homogeneous and periodic foundations, respectively, while cases *c* and *d* assess the same foundation types supported by soil. In all configurations, a torque T is applied directly to the rotor. Each periodic foundation comprises three unit cells (270 nodes in total, 90 per cell), and both homogeneous and periodic foundations are modeled as undamped.

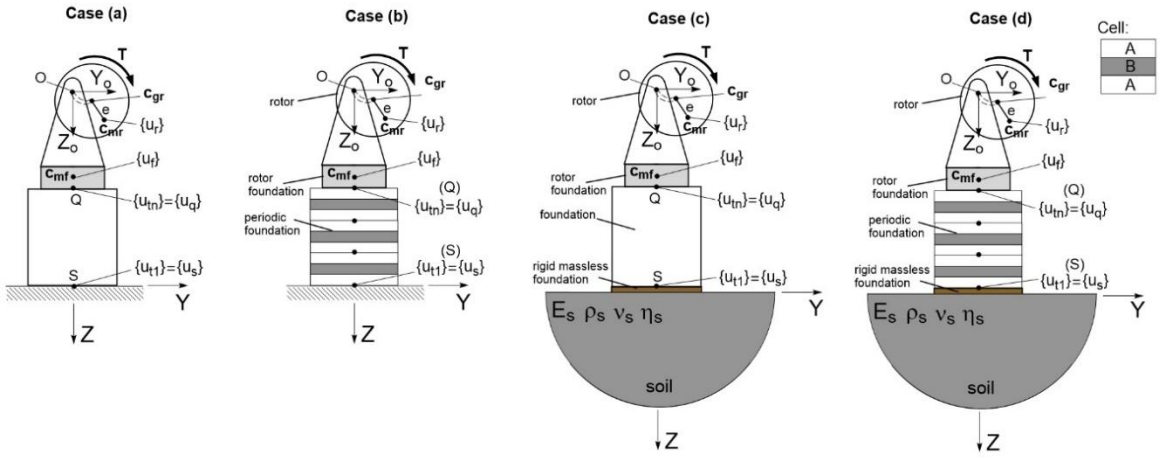


Figure 3. Cases for rotor-foundation-soil systems

Table 1 summarizes the material properties of the systems in Fig. 3. The steel rotor has a total mass m_D = 50 kg, unbalanced mass me=0.048 kg.m, shaft stiffness k_r = 904,778.7 N/m, damping coefficient c_r = 190.9 N.s/m, and natural frequency ω_r = 134.4 rad/s. The homogeneous foundation is made of material A (steel), whereas the periodic foundation combines material A (steel) and material B (rubber). The homogeneous half-space is modeled with typical soil properties: damping η = 0.01, Poisson's ratio ν = 0.3, and shear modulus G = 90 MPa. The soil's

vertical flexibility profile, $\{N_{Sz}(\omega)\}$, is shown in Fig. 2.

Table 1. System properties

Property	Unit cell - A (steel)	Unit cell - B (rubber)	Rotor (steel)	Half space
Young's Modulus (E)	210 GPa	3.2 GPa	210 GPa	234 MPa
Density (ρ)	7850 kg/m^3	1000 kg/m^3	7850 kg/m^3	2500 kg/m^3

The frequency response functions (FRFs) of Subsystem II (Fig. 1c), considering both homogeneous and periodic foundation configurations, are presented in Figs. 4 and 5. For the fixed-base scenarios (cases *a* and *b*), Fig. 4 shows the FRFs at node 2 (foundation base, Fig. 4a) and at the rotor-foundation interface (upper node, Fig. 4b). Fig. 5 presents the corresponding FRFs when the subsystem is coupled to a half-space (cases *c* and *d*), again at node 2 (Fig. 5a) and at the upper node (Fig. 5b). In both figures, the red curves, representing the foundation base FRFs, clearly display bandgaps. The presence of the soil induces attenuation and smoothing of resonant modes. This effect is less pronounced in case d at the rotor-foundation interface (Fig. 5b).

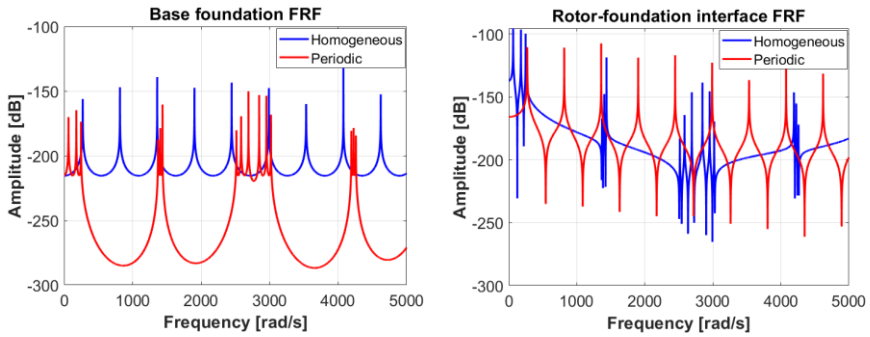


Figure 4. Foundation FRFs (homogeneous and periodic) - fixed base; (a) base foundation, (b) interface

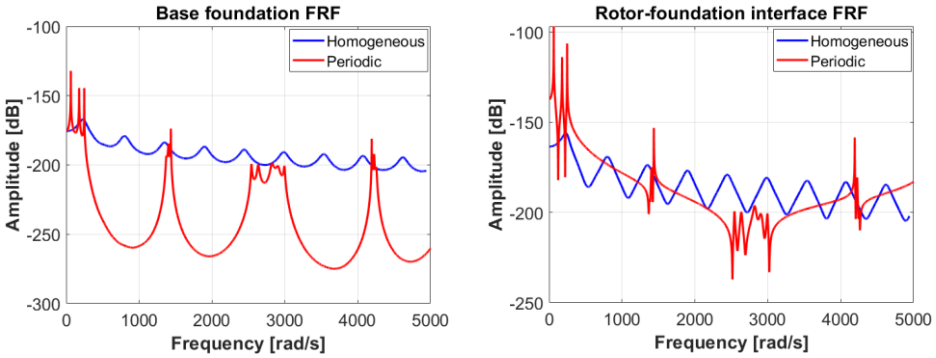


Figure 5. Foundation FRFs (homogeneous and periodic) - half space; (a) base foundation, (b) interface

Three modal parameters extracted from the FRFs of the homogeneous and periodic foundations with fixed base (Fig. 4), as well as those supported by the half-space (Fig. 5), are summarized in Tab. 2. Significant differences in natural frequencies are observed between cases *a* and *c* (homogeneous foundation) and cases *b* and *d* (periodic foundation), attributed to the presence of bandgaps. Furthermore, while the soil introduces damping in the homogeneous foundation (case *c*), this effect is minimal in the periodic configuration (case *d*).

Table 2. Modal parameters extracted for three DOFs of the analyzed systems

Case a	Case b	Case c		Case d	
Nat. Freq. (rad/s)	Nat. Freq. (rad/s)	Nat. Freq. (rad/s)	Damping F.	Nat. Freq. (rad/s)	Damping F.
$\omega_{n2} = 815.1$	$\omega_{n2} = 178.2$	$\omega_{n2} = 805.3$	$\xi_2 = 0.0687$	$\omega_{n2} = 177.7$	$\xi_2 = 0.0035$
$\omega_{n3} = 1358.5$	$\omega_{n3} = 248.1$	$\omega_{n3} = 1352.0$	$\xi_3 = 0.0410$	$\omega_{n3} = 247.4$	$\xi_3 = 0.0005$
$\omega_{n6} = 2989.0$	$\omega_{n6} = 1436.4$	$\omega_{n6} = 2985.8$	$\xi_6 = 0.0190$	$\omega_{n6} = 1436.4$	$\xi_6 = 0.0004$

Using the modal basis extracted for each case (Tab. 2), eq. (9) is defined and integrated together with the rotor subsystem equations (eqs. (1) to (3)). Applying the iterative coupling method yields the transient response of the coupled rotor-foundation-soil system. Figure 6 illustrates the vertical displacements of the rotor and foundation node 2 for case *d* under an applied torque of T = 30 Nm. Pronounced amplitude increases are observed near the rotor and periodic foundation resonance regions.

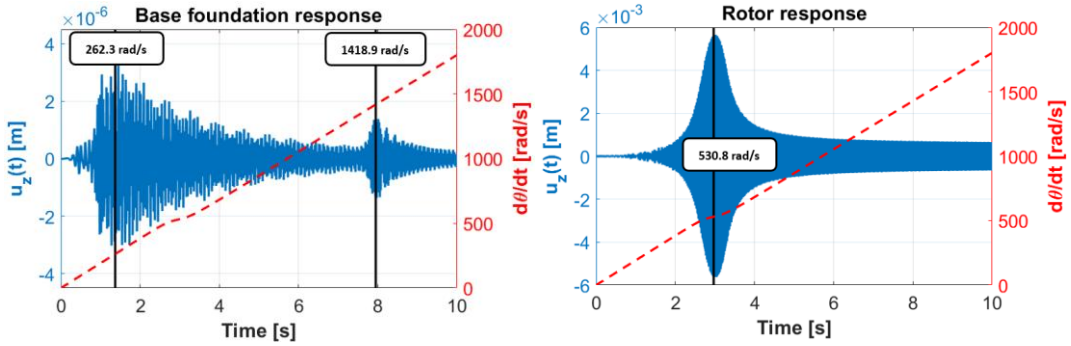


Figure 6. Rotor runup - Case d - T = 30 Nm

3.1 Minimum torque for each case

One analyzed scenario involves rotor acceleration through resonance, where vibration amplitudes and damping losses rise. If losses match or exceed the input energy, the rotor stalls at resonance. The minimum torque required to avoid this, T_{min}, is assessed for the four cases in Fig. 3 under two conditions: rotor natural frequency outside and inside the bandgap. Table 3 shows results for ω_r = 134.4 rad/s (outside the bandgaps, Figs. 4 and 5) and ω_r = 520.5 rad/s (increased shaft stiffness), centered within the first bandgap. In all cases (*a–d*), the stagnation speed closely matches the respective natural frequency. When ω_r lies outside the bandgap, soil damping in the homogeneous foundation (cases *a* and *c*) reduces both the response amplitude, u_{rz}, and T_{min} , with smaller reductions observed for the periodic foundation (cases *b* and *d*). Within the bandgap, the soil has no influence on the periodic cases (*b* and *d*), as reflected in unchanged T_{min} and u_{rz} values.

Table 3. Torque limit and maximum displacement - Rotor

Rotor natural frequency - ω_{nr} = 134.4 rad/s			
Case a	Case b	Case c	Case d
T_{min} = 19.87 Nm u_{rz} = 0.04198 m	**T_{min} = 19.26 Nm** **u_{rz} = 0.04211 m**	T_{min} = 19.64 Nm u_{rz} = 0.03916 m	**T_{min} = 19.20 Nm** **u_{rz} = 0.04135 m**
Rotor natural frequency - ω_{nr} = 520.5 rad/s			
Case a	Case b	Case c	Case d
T_{min} = 18.81 Nm u_{rz} = 0.00575 m	**T_{min} = 18.53 Nm** **u_{rz} = 0.00556 m**	T_{min} = 18.60 Nm u_{rz} = 0.00562 m	**T_{min} = 18.53 Nm** **u_{rz} = 0.00556 m**

3.2 Base foundation transient response (Cases *a-d*)

Focusing on the condition where ω_r = 520.5 rad/s lies within the bandgap, the transient responses of foundation node 2 (base node) in cases *a–d* are compared under their respective minimum torque values (Tab. 3). Figure 7 shows the responses during rotor acceleration until stagnation. For rigid foundations, case *a* exhibits larger displacement than case *b*, while with soil support, case *c* exceeds case *d*. The periodic foundation reduces displacement magnitudes and effectively suppresses soil influence: the largest amplitude occurs in case *c* (homogeneous foundation with soil), whereas case *d* (periodic foundation with soil) shows amplitudes similar to rigid-base cases.

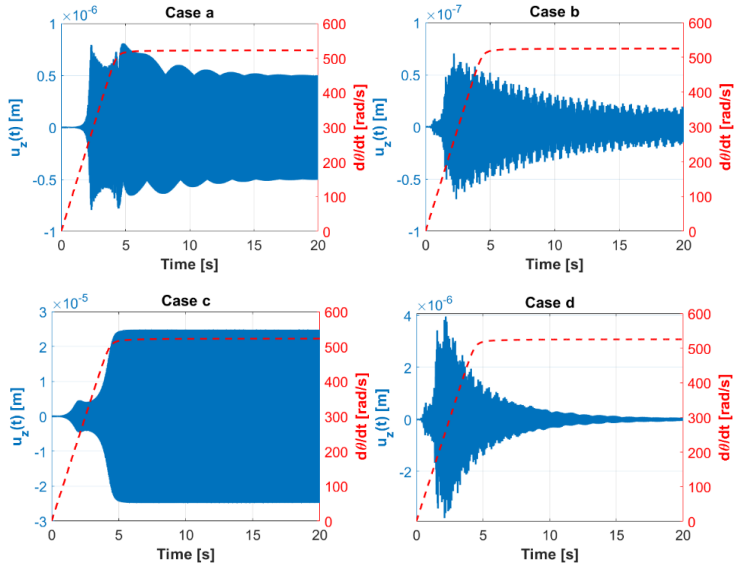


Figure 7. Base foundation response (node 2)

4 Conclusions

This study presents a methodology for analyzing the transient behavior of rotor–foundation–soil systems, enabling accurate solutions for a nonlinear system coupled to another exhibiting geometric damping, as in unbounded domains. The analyzed cases show that introducing a periodic foundation can alter the rotor's dynamic response, potentially nullifying the soil's geometric damping effects when the rotor's natural frequency lies within the foundation's bandgaps.

Acknowledgements. The research leading to this work was funded by the São Paulo Research Foundation (Fapesp) grant FAPESP CEPID Process 2013/08293-7 and Coordination for the Improvement of Higher Education Personnel - Brazil (CAPES) - Finance Code 001. The support of CNPq and Faepex/Unicamp is also gratefully acknowledged.

Authorship statement. The authors hereby confirm that they are the sole liable persons responsible for the authorship of this work, and that all material that has been herein included as part of the present paper is either the property (and authorship) of the authors, or has the permission of the owners to be included here.

References

[1] Kellezi, L.; Hansen, P. B. "Dynamic transient analysis of a mono-pile windmill foundation". Proceedings of *EURODYN, 4th Int. Conference on Structural Dynamics*. Munich, Germany. pp. 1315-1320, 2002.
[2] Xiang, H. J.; Shi, Z. F., Wang, S. J. and Mo, Y. L. "Periodic materials-based vibration attenuation in layered foundations: experimental validation". Smart Materials and Structures, IOP Publishing Ltd, 2012.
[3] Felippa C. A. and Park K. C. "Staggered transient analysis procedures for coupled mechanical systems: formulation". Computer Methods in Applied Mechanics and Engineering, Vol. 24, Issue 1, pp. 61-111, 1980.
[4] Carrion, R.; Sousa, A. D. O. and Mesquita, E. "The influence of soil damping mechanisms and geo-profiles on the stationary response of 3d rigid block foundations". In Proceeding of *19th International Congress of Mechanical Engineering*, 2007.
[5] Ferraz, A. C.; Mesquita; E. and Pacheco, L. A. "Dynamics of a rotor-structure-soil system: transient response by iterative coupling". Latin American Journal of Solids and Structures, 2025. (Submitted)
[6] Pacheco, L.A.; Ferraz, A. C.; Mesquita, E. and Lima, L. F. V. "Transient response of bar structures interacting with layered soil profiles". In Proceedings of the *9th International Symposium on Solid Mechanics, MECSOL2024*, 2024.
[7] Cook, R. D.; Malkus, D. S.; Plesha, M. E. and Witt, R. J. *Concepts and Applications of Finite Element Analysis*. 4th ed., John Wiley and Sons, New York, 2005.
[8] Ferraz, A. C.; Pacheco, L. A.; Carrion, R. and Mesquita, E. "Coupling Modal Analysis with the BEM for the Transient Response of Bar Structures Interacting with Three-Dimensional Soil Profiles". LAJSS, Vol. 20 No. 6, 2023.
[9] Ewins, D.J. *Modal testing: theory, practice and application*. Wiley, New York, 2000.